Volume 46 | Number 46 | 14 December 2017 | Pages 15965–16328

Dalton Transactions

An international journal of inorganic chemistry

rsc.li/dalton

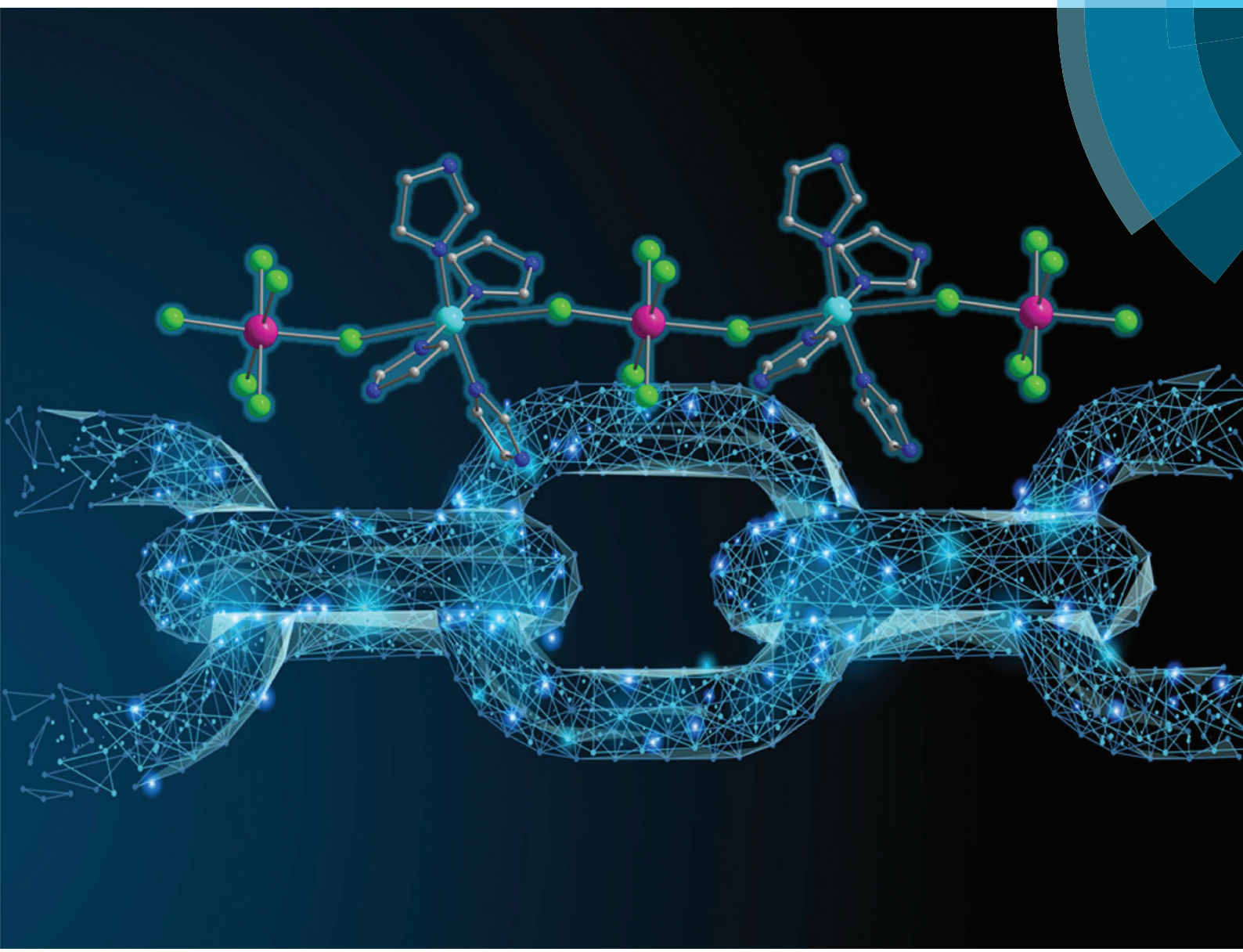

ISSN 1477-9226

ROYAL SOCIETY OF CHEMISTRY

PAPER

José Martínez-Lillo, Joan Cano, Euan K. Brechin *et al.*

Magneto-structural correlations in a family of $Re^{IV}Cu^{II}$ chains based on the hexachlororhenate(IV) metalloligand

Dalton Transactions

PAPER

View Article Online
View Journal | View Issue

Cite this: *Dalton Trans.*, 2017, **46**, 16025

Magneto-structural correlations in a family of $Re^{IV}Cu^{II}$ chains based on the hexachlororhenate(IV) metalloligand†

Anders H. Pedersen, [a] Miguel Julve, [b] José Martínez-Lillo, *[b] Joan Cano *[b] and Euan K. Brechin *[a]

Received 19th June 2017,
Accepted 24th July 2017

DOI: 10.1039/c7dt02216f

rsc.li/dalton

Six novel one-dimensional chloro-bridged $Re^{IV}Cu^{II}$ complexes of formula $\{[Cu(L)_4][ReCl_6]\}_n$, where L = imidazole (Imi, **1**), 1-methylimidazole (Meim, **2**), 1-vinylimidazole (Vim, **3**), 1-butylimidazole (Buim, **4**), 1-vinyl-1,2,4-triazole (Vtri, **5**) and *N*,*N*′-dimethylformamide (DMF, **6**) are characterised structurally, magnetically and theoretically. The structures exhibit significant differences in Cu–Cl bond lengths and Re–Cl–Cu bridging angles, resulting in large differences in the nature and magnitude of magnetic exchange interactions between the Re^{IV} and Cu^{II} ions. Theoretical calculations reveal the coupling to be primarily ferromagnetic, increasing in magnitude as the bridging angle becomes smaller and the bond lengths shorten.

Introduction

The ability of the synthetic chemist to design and manufacture molecule-based magnetic materials conforming to specific architectures and topologies, whilst controlling symmetry, metal geometries and metal–ligand interactions, is key to the commercial applicability of such species in, for example data storage and spintronics.[1] This effort relies upon the systematic study of large families of closely related compounds such that the relationship between structure and magnetic properties can first be quantitatively understood, and second be exploited and improved through bottom-up, controlled chemical manipulation at the molecular scale.[2]

In this context, the most studied transition metal molecule-based magnets are polynuclear complexes based on paramagnetic 3d ions.[2e] In comparison, systems containing the heavier 4d and 5d ions have been much less explored, despite these metal ions being characterised by more radially extended magnetic orbitals (5d > 4d ≫ 3d) which results in larger spin delocalisation onto coordinated atoms/ligands creating stronger magnetic exchange between paramagnetic metal ions.[3–5] The extremely large spin–orbit coupling constants (λ) of 4d and 5d ions is a direct cause of their unusually large zero-field splitting (zfs) values manifested in the axial (D) and rhombic (E) components, and highly anisotropic g-factors.[4] Zero-field splitting plays an important role in the energy barrier for reversal of the magnetisation in these systems, and for this reason the $5d^3$ Re^{IV} ion is of great interest due to its large magnetic anisotropy,[5] which arises from second order spin–orbit coupling caused by a spin–orbit coupling constant for the free ion of $\lambda \approx 1000$ cm^{-1}.[6] Apart from investigations into the magnetic properties of its salts (*e.g.* the effect of cation size on intermolecular interactions and T_c), the role of the $[ReCl_6]^{2-}$ anion has been largely limited to that of synthetic precursor.[6–19] Indeed, a common strategy for the creation of new Re^{IV} complexes is the functionalisation of the $[ReCl_6]^{2-}$ anion through halide exchange with ligands such as heterocyclic amines, pseudo halides such as cyanide, or chelates such as the oxalate anion.[6,10–13] These species have subsequently been employed as metalloligands for the creation of larger oligomers.[14–17] More recently, several 1D chains based on the Re^{IV} ion have been reported. For example, the $[trans\text{-}ReCl_4(CN)_2]^{2-}$ anion was used to construct the Single-Chain Magnet (SCM) $\{[Fe(DMF)_4][trans\text{-}ReCl_4(CN)_2]\}_n$ which displays a coercive field of 1 T at T = 1.8 K,[9] the $[ReF_6]^{2-}$ anion was used for the first time in 2014 as a metalloligand for the synthesis of the 1D complex $\{[Ni(Vim)_4][ReF_6]\}_n$ which exhibits strong ferromagnetic exchange between neighbouring metal ions,[20] while the $\{[Cu(pyim)_2][ReCl_4(ox)]\}_n$ chain (pyim = 2-(2′-pyridyl)imidazole and ox = oxalate) exhibits ferrimagnetic behaviour due to the presence of two different magnetic exchange interaction

[a]*EaStCHEM School of Chemistry, The University of Edinburgh, David Brewster Road, EH9 3FJ Edinburgh, UK. E-mail: E.Brechin@ed.ac.uk*
[b]*Departament de Química Inorgànica/Instituto de Ciencia Molecular (ICMol), Universitat de València, C/Catedrático José Beltrán 2, Paterna, València, Spain. E-mail: joan.cano@uv.es, F.Jose.Martinez@uv.es*

†Electronic supplementary information (ESI) available: Crystallographic, structural and magnetic data. CCDC 1550271–1550276. For ESI and crystallographic data in CIF or other electronic format see DOI: 10.1039/c7dt02216f

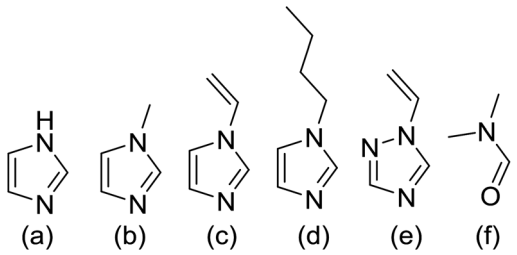

Scheme 1 The ligands (L) employed: (a) imidazole, (b) 1-methylimidazole, (c) 1-vinylimidazole, (d) 1-butylimidazole, (e) 1-vinyl-1,2,4-triazole, (f) dimethylformamide.

pathways (O, Cl) between the Re^{IV} and Cu^{II} ions.[21] The possibility of using the $[ReCl_6]^{2-}$ unit as a linker for neutral chains was introduced recently with the study of the species $\{[Cu(pyim)(Imi)_2][ReCl_6]\}_n$ (Imi = imidazole) which revealed antiferromagnetic exchange interactions and metamagnetic behaviour.[22]

This latter discovery has prompted us to search for more 1D networks based on the $[ReCl_6]^{2-}$ anion, and herein we present six new chains which are characterised structurally, magnetically and theoretically. These chains are of general formula $\{[Cu(L)_4][ReCl_6]\}_n$, where L = imidazole (Imi, **1**), 1-methylimidazole (Meim, **2**), 1-vinylimidazole (Vim, **3**), 1-butylimidazole (Buim, **4**), 1-vinyl-1,2,4-triazole (Vtri, **5**) and *N*,*N*′-dimethylformamide (DMF, **6**) (Scheme 1). The structures exhibit significant differences in Cu–Cl bond lengths and Re–Cl–Cu bridging angles, originating from the differences in the identity of the ligands (L) terminally bonded to the Cu^{II} ion. Combined with a theoretical examination of the magneto-structural relationship, a clear design principle for the construction of ferro- or antiferromagnetically coupled Re^{IV}–Cu^{II} chains emerges.

Results and discussion

The structures of complexes **1–6** (Fig. 1 and Fig. S1–S15, Tables S1–S4†) are similar and describe a motif of alternating $[ReCl_6]^{2-}$ and $[Cu(L)_4]^{2+}$ units linked by *trans* chloride ions, thereby creating 'zig-zag' 1D chains. The $[ReCl_6]^{2-}$ anion contains a slightly disordered octahedral geometry with Re–Cl bond lengths in the range 2.3457(5)–2.3859(4) Å, in accordance with previously published compounds containing this moiety (Tables S3 and S4†).[5,7] The Cu^{II} ion sits in a *trans*-X_4Cl_2 coordination sphere (X = N (**1–5**) or O (**6**)) with the chloride ions positioned along the Jahn–Teller (JT) axis, with Cu–N bond lengths of 1.979(3)–2.017(2) Å for **1–5** and Cu–O bond lengths of 1.9450(16) and 1.9609(16) Å in **6** (Cu–O(2), Cu–O(1), respectively). Despite these similarities, the Cu–Cl bond lengths and the Re–Cl–Cu bond angles vary enormously, with Cu–Cl distances ranging between 2.78–3.23 Å, and the Re–Cl–Cu bond angles being as small as 128.6° and as large as 152.8° (Tables S3 and S4†). A search of the Cambridge Structural Database (CSD) reveals that Cu–Cl bond distances in previously published Cu–Cl–TM (TM = transition metal) 1D chains range

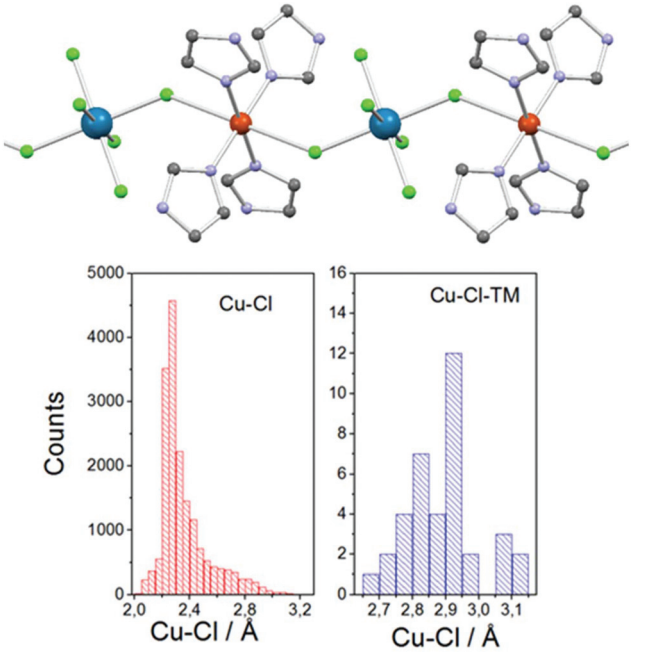

Fig. 1 The $\{[Cu(L)_4][ReCl_6]\}_n$ chain motif common to compounds **1–6**. The figure shown is compound **1** (top). The Cu–Cl distances range between 2.78–3.23 Å, the Re–Cl–Cu bond angles lie between 128.6–152.8°. Hydrogen atoms and solvent molecules omitted for clarity. Colour code: Re, cyan; Cu, brown; Cl, green; O, red; N, blue; C, grey. Bar graphs showing the range of all Cu–Cl distances reported in the CSD (bottom left), and all those in previously published Cu–Cl–TM compounds containing a μ-bridging Cl^- ion (bottom right).

from ~2.6–3.2 Å, putting those observed in **1–6** at the very top end. There is no 'simple' explanation as to the origin of the ~24° difference in the bridging angle at the chloride ion, but the size/steric bulk of the ligand (L) terminally bonded to the Cu^{II} ion, in concert with the associated effects on intermolecular interactions in the extended structure, are likely the most dominant parameters (Tables S3 and S4†).

The chains crystallise in the triclinic space group $P\bar{1}$ (**1**, **2** and **6**), monoclinic space groups $C2/c$ (**3**) and $P2_1/c$ (**5**), and the orthorhombic space group *Pccn* (**4**) (Tables S1 and S2†). The asymmetric unit (ASU) of **1** contains two non-equivalent half molecules of the $[Cu(Imi)_4]^{2+}$ cation, one $[ReCl_6]^{2-}$ anion and two isopropanol molecules (Fig. S1†). In **2**, the ASU contains 1.5 molecules of the $[Cu(Meim)_4][ReCl_6]$ motif, giving rise to two non-equivalent chains whose structural parameters deviate slightly (Fig. S2†). The ASUs of **3–6** contain half a cation and half an anion due to inversion centres located on the Re^{IV} and Cu^{II} metal ions (Fig. S3–6†). One solvent acetonitrile molecule at 50% occupancy is also part of the ASU of **6**.

In the crystal lattice of **1**, the chains are oriented in a parallel fashion, and pack in layers in the crystallographic *bc* plane through C(H)···π interactions of ~3.5 Å (C-atom to imidazole centroid) and N(H)···Cl interactions of ~3.2 Å (Fig. S7†). The co-crystallised isopropanol molecules pack through O(H)···O and N(H)···O hydrogen bonds in the crystallographic *bc* plane between layers of chains. In the extended structure of **2**, the

chains travel parallel to the crystallographic *b* axis and pack *via* a range of C(H)···π, Cl···π and Cl···Cl interactions. Adjacent $[Cu(Meim)_4]^{2+}$ units pack through C(H)···π interactions of ~3.6–3.8 Å, with the $[ReCl_6]^{2-}$ anions packing through Cl···π (intra- and inter-chain) and Cl···Cl (inter-chain) interactions (Fig. S8†). The $[ReCl_6]^{2-}$ anions have short Cl···π interactions of ~3.6–3.8 Å to the cations and inter-chain Cl···Cl interactions of ~3.9 Å between anions (Fig. S8b†).

The chains in **3** are ordered in 2D networks in the crystallographic *ab* plane, with each 2D network being pseudo-perpendicular to adjacent layers at an inter-chain angle of 81.45° (Fig. S9†). The chains pack through an extended network of Cl···π and C(H)···π interactions, with the shortest intra- and inter-chain Cl···π/C(H)···π interactions being approximately 3.4 Å and 3.6–3.9 Å, respectively (Fig. S10†). In **4**, the chains describe a 'grid' like pattern down the crystallographic *c* axis (Fig. S11†). Each chain is well isolated from its nearest neighbours on account of the bulkiness of the butyl group of the imidazole ligands, which causes the inter-chain metal···metal distances to be >9 Å.

In the crystal lattice of **5**, the chains propagate down the crystallographic *a* axis and pack through a myriad of intra- and inter-chain C(H)···N and Cl···π interactions. In each neutral chain, two short Cl···π interactions of ~3.4 and ~3.7 Å are present (Fig. S12a†) with the chains packing through short inter-chain C(H)···N interactions between triazole groups, and Cl···π interactions from the anions to the vinyl groups (Fig. S12b†). These C(H)···N interactions are of the order 3.2 Å, with inter-chain Cl···π distances of approximately 3.6 Å. The molecular chains of **6** are oriented in a parallel manner down the crystallographic *c* axis, with the acetonitrile molecules of crystallisation in the voids between the chains (Fig. S13†). The $[ReCl_6]^{2-}$ unit interacts with the DMF ligands and acetonitrile solvate molecules through C(H)···Cl contacts, with C···Cl distances in the range of 3.5 to 3.8 Å (Fig. S14a†). C(H)···N interactions link the DMF ligands with the acetonitrile molecules, with C···N distances of approximately 3.3 and 3.6 Å (Fig. S14b†).

Magnetic behaviour

Plots of the $\chi_M T$ product *versus* *T* in the temperature range *T* = 300–2 K for complexes **1–6** are shown in Fig. 2; where χ_M is the molar magnetic susceptibility for a $Re^{IV}Cu^{II}$ unit. The $\chi_M T$ values at room temperature (1.86–1.95 $cm^3\ mol^{-1}\ K$) are close to that expected for one *S* = 3/2 ion and one *S* = 1/2 ion, with *g*-factors equal to 1.8 and 2.1, respectively. In the *T* = 300–100 K temperature region complexes **1–6** display very similar behaviour, with little change in the magnitude of $\chi_M T$ being observed. At lower temperatures the data deviate, the differences being due to different magnetic exchange (in both magnitude and sign) between the spins on the Re^{IV} and Cu^{II} ions, together with the zfs associated with the Re^{IV} ion.[5] For **1**, $\chi_M T$ falls to 1.37 $cm^3\ K\ mol^{-1}$ at *T* = 5.5 K, before rising to 6.28 $cm^3\ K\ mol^{-1}$ at *T* = 2.0 K. For complexes **2**, **4** and **6** the $\chi_M T$ product continually decreases, reaching values of 1.45, 1.28 and 1.74 $cm^3\ K\ mol^{-1}$ at *T* = 2.0 K, respectively. Complexes

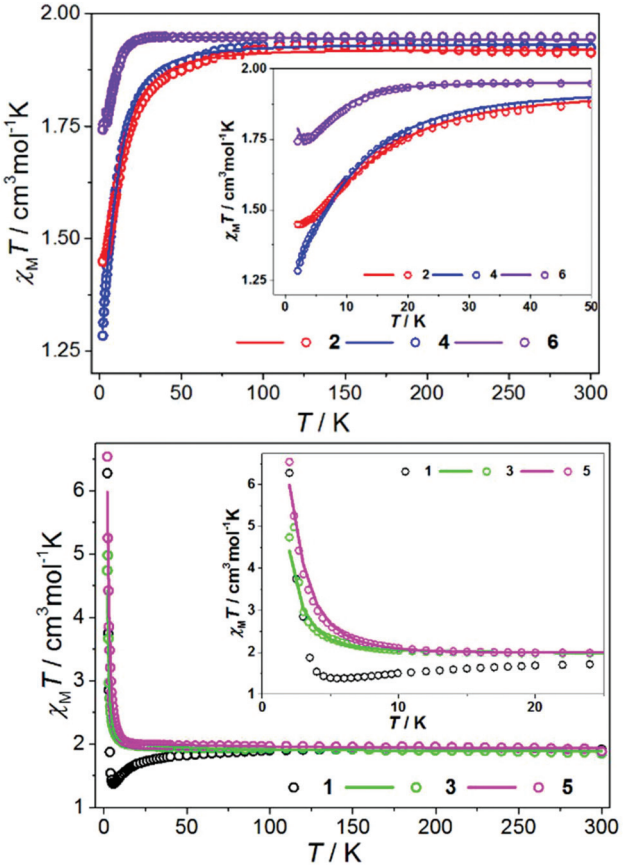

Fig. 2 Plot of the $\chi_M T$ product *versus* *T* for complexes **2**, **4**, **6** (top) and **1**, **3**, **5** (bottom). The insets show a blow-up of the low temperature region. Solid lines are a fit of the experimental data (empty circles). See text for details.

3 and **5** display analogous behaviour: $\chi_M T$ increasing slowly between *T* = 100–12 K before increasing more rapidly between 12–2 K and reaching maximum values of 4.98 and 6.54 $cm^3\ K\ mol^{-1}$ at *T* = 2.4 and 2.0 K, respectively.

Quantitative analysis of the magnetic behaviour of Re^{IV} compounds is non-trivial, since one must consider both intra- and inter-molecular exchange interactions caused by the strong delocalisation of spin density from the Re^{IV} ion to the coordinated ligands (the latter can be as strong as the former), different *g*-values for the constituent metal ions (g_{Re} and g_{Cu}), and zero-field splitting effects (D_{Re}).[5] In addition we note that some of these parameters are correlated: for example, erroneously large antiferromagnetic intra- or inter-molecular exchange can be deduced at the expense of underestimating zfs, whilst large ferromagnetic exchange is linked to an overestimation of zfs. It is therefore important than any employed model be as simple as possible. In this respect, we have carried out DFT calculations to estimate the magnitude of the exchange through the shortest inter-molecular contacts between $[ReCl_6]^{2-}$ moieties in all six complexes. These values, together with the shortest Re···Re, Re···Cu, and Cl···Cl distances between adjacent chains are collected in Table 1.

Table 1 Inter-molecular distances between adjacent chains and the magnetic coupling constants for the shortest inter-molecular contacts

Compound	d(Re···Re)/Å	d(Re···Cu)/Å	d(Cl···Cl)/Å	J/cm^{-1}
1	7.87	8.05	3.80	−0.023
			6.87	+0.000
2	8.18	7.71	3.86	+0.027
			4.29	+0.004
3	9.22	8.83	5.425	+0.001
			6.55	+0.000
			6.59	+0.004
4	10.73	9.33	7.01	+0.000
			7.67	+0.000
5	8.75	9.74	4.64	+0.003
6	8.46	9.49	5.22	+0.007
			5.34	+0.006

DFT calculations show that the inter-chain magnetic exchange interactions in **1–6** are negligible, even in the cases of complexes **1** and **2** where the Cl···Cl contacts are relatively short (Table 1). The magnetic behaviour of **1–6** can therefore be regarded as originating from isolated heterometallic 1D chains.

The magnetic properties of certain homo- and heterometallic Re^{IV} based complexes have previously been studied using an approach that considers only the lowest-lying Kramers doublet is populated at low temperature, rendering the ion an effective spin doublet (S_{eff} = 1/2).[5] However, this approach is only useful when $D_{Re} \gg J_{ReCu}$ (by at least one order of magnitude). In most cases involving pseudohalide $[ReX_6]^{2-}$ ions this condition is not met, and the analytical methodology required for implementing this approach becomes rather complex.[23] In order to verify our starting point, we have therefore performed a NEVPT2 calculation of the axial (D) and rhombic (E) components of the zfs tensor of the $[ReCl_6]^{2-}$ ion in complex **1**. The results afford g = 1.761, D = −8.0 cm^{-1}, and E/D = 0.163, confirming the presence of a moderate axial component of the magnetic anisotropy ($D_{Re} \approx J_{ReCu}$). Thus an approach based on the exact diagonalization of the energy matrix of a $\{Re^{IV}Cu^{II}\}_n$ wheel, has been employed. The weak magnetic exchange between the metal ions, clearly observed in the susceptibility data, allows us to use a model wheel that incorporates just eight metal centres (Fig. 3). The magnetic coupling between the paramagnetic centres is described as the sum of the Zeeman ($\hat{H}_{Zeem}$), zero-field splitting ($\hat{H}_{zfs}$) and Heisenberg magnetic coupling ($\hat{H}_{Heis}$) contributions, where B is the applied magnetic field and β the Bohr magneton:

$$\hat{H}_{Zeem} = \sum_{n=0}^{3} (g_{Re}\hat{S}_{2n+1} + g_{Cu}\hat{S}_{2n+2})B\beta$$

$$\hat{H}_{zfs} = \sum_{n=0}^{3} \Big(D[(\hat{S}^{z}_{2n+1})^2 - S_{2n+1}(S_{2n+1}+1)/3] + E[(\hat{S}^{x}_{2n+1})^2 - (\hat{S}^{y}_{2n+1})^2] \Big)$$

$$\hat{H}_{Heis} = \sum_{n=1}^{7} -J\hat{S}_n\hat{S}_{n+1} + J\hat{S}_1\hat{S}_8$$

The theoretical curves obtained using this spin-Hamiltonian are shown in Fig. 4.[5] Positive and negative values for D_{Re} and J were used to identify the effects on the thermal dependence of the magnetic susceptibility. When there is zero coupling between the metal ions the magnetic behaviour does not depend on the sign of the axial zfs parameter, and the $\chi_M T$ value decreases to a non-zero value at T = 0 K ($\chi_M T_0$). If the exchange coupling is non-zero, the magnetic behaviour is affected by the sign of D_{Re}, but only at very low temperatures. For example, when the neighbouring spins are antiferromagnetically coupled, the $|\pm 3/2\rangle$ Kramers doublet of the Re^{IV} ion is coupled with the $|\pm 1/2\rangle$ doublet of the Cu^{II} ion for $D_{Re} < 0$. In such a scenario, the spins do not cancel and an increase in $\chi_M T$ is observed at low temperatures, leading to values slightly larger than $\chi_M T_0$. For $D_{Re} > 0$, the spin of the $|\pm 1/2\rangle$ ground Kramers doublet on the Re^{IV} ion can be 'cancelled out' by coupling to the Cu^{II} ion, though the curve is also dependent on the different g-factors. Thus, a continuous decrease of $\chi_M T$ occurs to values lower than the $\chi_M T_0$ limit. When the exchange is ferromagnetic, $\chi_M T$ increases with decreasing temperature, diverging at low temperature towards a non-finite value, as expected for an ideal one-dimensional system. For small J/D_{Re}

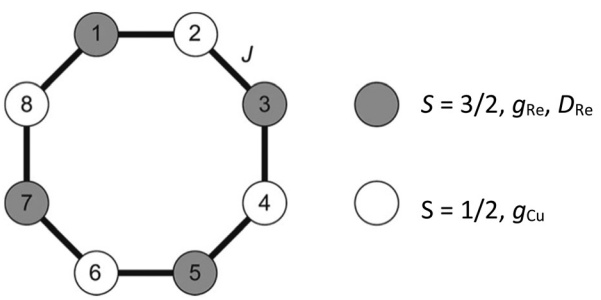

Fig. 3 Spin topology of the model used to simulate the magnetic behaviour of compounds **1–6**.

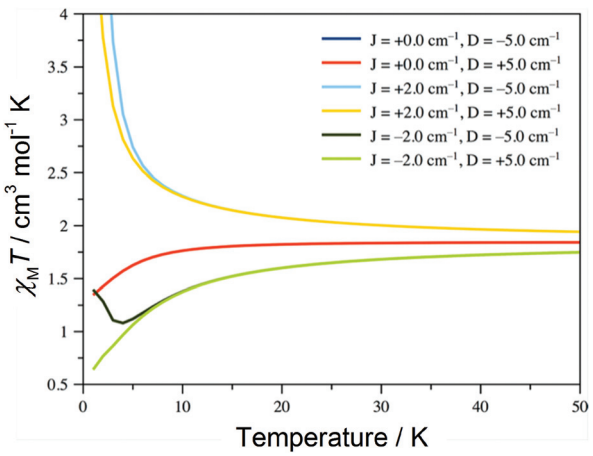

Fig. 4 Theoretical thermal dependence of the $\chi_M T$ product for the model schematised in Fig. 3 for different values of J and D (inset). The dark red line (J = 0 cm^{-1}, D = +5 cm^{-1}) is directly superimposed on the dark blue line (J = 0 cm^{-1}, D = −5 cm^{-1}).

ratios a small decrease in $\chi_M T$ is observed leading to values at low temperatures that are greater than $\chi_M T_0$.

We can therefore extract some qualitative conclusions from the experimental thermal dependence of $\chi_M T$ in Fig. 2. The continuous decrease of the $\chi_M T$ value to values close to $\chi_M T_0$ for complexes **2**, **4** and **6** suggest that the magnetic coupling in these compounds could be ferro- or antiferromagnetic, but very weak in each case. The higher $\chi_M T$ values at T = 2 K in **2** and **6**, suggest these systems possess a small but non-negligible ferromagnetic coupling. The greater decrease in $\chi_M T$ in **4** indicates the presence of antiferromagnetic exchange, whilst the sharp increase in $\chi_M T$ at low temperatures in **1**, **3** and **5** is evidence of ferromagnetic exchange interactions. The minimum in the $\chi_M T$ value close to the $\chi_M T_0$ limit observed in **1** points to a smaller J/D_{Re} ratio than detected in **3** and **5**.

In order to support these qualitative conclusions, and to establish which structural parameters govern the nature and magnitude of the magnetic exchange coupling (Fig. 5), we have theoretically estimated J from DFT calculations on a $[Re^{IV}Cu^{II}_2]$ fragment (Table 2 and Fig. S15†). We note the following points: (a) complexes **1** and **2** each contain two distinct coupling constants (derived from two different geometries), assigned **X_1** and **X_2**; (b) two different $Re^{IV}Cu^{II}$ chains coexist in **2**, named **2a** and **2b**; the exchange is weak and mediated *via* the axial JT axis of the Cu^{II} ion. Thus the results should be regarded as semi-quantitative with some leeway allowed for the estimated J values.

As predicted from the theoretical simulations (Fig. 4), the strongest ferromagnetic exchange interactions are observed in complexes **3** and **5** (Table 2). Ferromagnetic and antiferromagnetic exchange co-exists in **1**, the former stronger than the latter, in agreement with the observed experimental data. The weakest interactions in the family are observed in **2** and **4**. The average value of J in **2** is consistent with the experimental data, showing a tendency for $\chi_M T$ to increase at temperatures close to T = 2 K. A comparison of the J values with the Re–Cl–Cu bond angle, α, shows the coupling to become more ferromagnetic with a smaller bridging angle (Fig. S16†). As expected, the second-neighbouring Cu–Cu magnetic coupling is zero in all calculated $[Re^{IV}Cu^{II}_2]$ fragments.

In order to establish a magneto-structural correlation for this family of complexes we have examined how the strength of the exchange varies with the Cu–Cl distance (d(Cu–Cl)), the Cu–Cl–Re angle (α), and the twist of the $[ReCl_6]^{2-}$ moiety around the JT axis of the Cu^{II} ion (θ), using the model complex shown in Fig. 5. The d(Cu–Cl) bond length and the α and θ angles have been varied between 2.50–3.25 Å, 125 to 155°, and 0–45°, respectively. The results are summarized in the 2D contour maps shown in Fig. 6 and S17–S19.† The results confirm our previous conclusions: (1) the magnetic exchange is weak in all cases; (2) they are mainly ferromagnetic in nature; (3) the magnitude of the coupling strongly depends on the α angle, but only slightly on the θ angle; (4) the axial Cu–Cl bond length strongly modifies the magnitude of the magnetic coupling; the shorter the bond the stronger the exchange. This last point is clear from Fig. 7 for two pairs of α and θ values.

The Cu^{II} ion has a unique magnetic orbital on its basal plane ($d_{x^2-y^2}$), with the Re^{IV} ion having all three t_{2g} orbitals

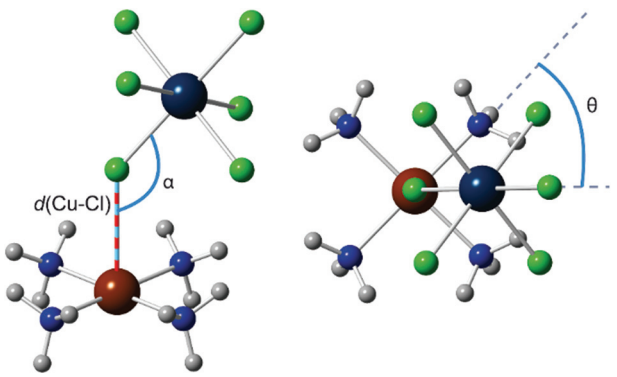

Fig. 5 Perpendicular (left) and parallel (right) views of the Jahn–Teller axis of the Cu^{II} ion in a $Re^{IV}Cu^{II}$ fragment, highlighting the Cu–Cl distance (d(Cu–Cl)), the Cu–Cl–Re angle (α), and the twist of the $ReCl_6$ moiety around the JT axis of the Cu^{II} ion (θ). Colour code as Fig. 1.

Table 2 Pertinent experimental structural data for complexes **1–6** (d(Cu–Cl), α, and θ, see Fig. 5) together with the calculated magnetic coupling constants (J) derived from the $[ReCu_2]$ models

Coupling	d(Cu–Cl)/Å	α/°	θ/°	J/cm^{-1}
1_1	3.058	148.59	41.68	−0.37
1_2	2.993	152.79	26.41	+0.57
2a	3.045	146.71	19.92	+0.29
2b_1	3.195	143.60	43.42	+0.64
2b_2	3.038	140.03	42.68	+0.71
3	2.883	132.99	9.43	+2.38
4	3.226	142.25	8.22	+0.31
5	2.857	128.66	39.15	+2.53
6	2.780	142.92	17.35	+0.68

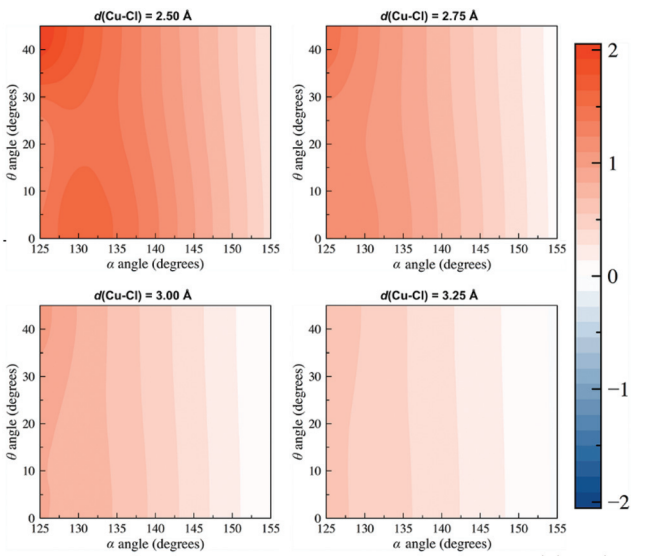

Fig. 6 Contour maps of the dependence of the α and θ angle on the magnetic coupling constant in the molecular model of Fig. 5 for several Cu–Cl bond lengths in the range 2.50–2.75 Å at regular intervals of 0.25 Å. The J value (cm^{-1}) range is indicated by the colour graded bar.

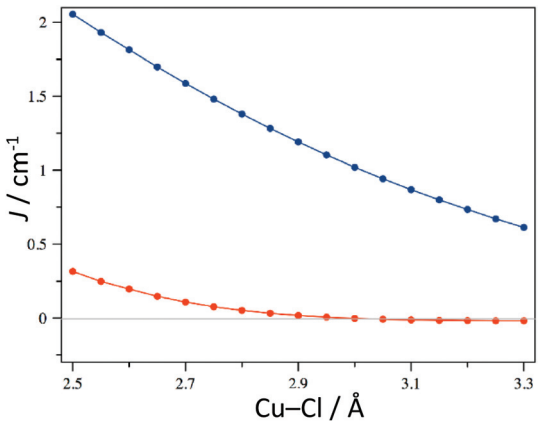

Fig. 7 Dependence of the Cu–Cl bond length on the magnetic coupling for the geometries ({α, θ}) {125°, 45°} (blue) and {155°, 45°} (red).

half-filled. Of these, the d_{xz} and d_{yz} magnetic orbitals delocalize their spin densities to the p_x and p_y orbitals of the bridging chloride ion; the d_{xy} magnetic orbital does not. The former are therefore the only magnetic orbitals to interact with the magnetic orbital of the Cu^{II} ion. A schematic evolution of this interaction is shown in Fig. 8. From this picture, it is clear to see that the contribution caused by the interaction between the d_{xz} orbital on the Re^{IV} ion and the $d_{x^2-y^2}$ orbital on the Cu^{II} ion should be ferromagnetic, and invariant with α (Fig. 8).[24,25]

Because of zero orbital overlap, the contribution promoted by the d_{yz} magnetic orbital should also be ferromagnetic. For smaller angles of θ this contribution should become larger, due to the increased interaction between the spin densities on the magnetic orbitals, despite orbital overlap remaining zero. The strong dependence of the Cu–Cl bond length on the magnetic exchange is clear from Fig. 7, and can be understood by a decrease in the interaction between the spin densities when this distance increases. Thus complexes **3** and **5** exhibit the strongest ferromagnetic coupling. Note that the theoretical exchange couplings are slightly more ferromagnetic than the experimental ones.

With the theoretical study as a guide, we then attempted to use our model to fit the experimental susceptibility data (Fig. 2), and obtained good simulations with the set of parameters given in Table 3. The analysis for compound **1** was excluded due to the presence of multiple coupling pathways. The experimental behaviour is in agreement with the calculated magnetic coupling constants, and the J values in Table 3 agree well with those in Table 2 and Fig. 9.

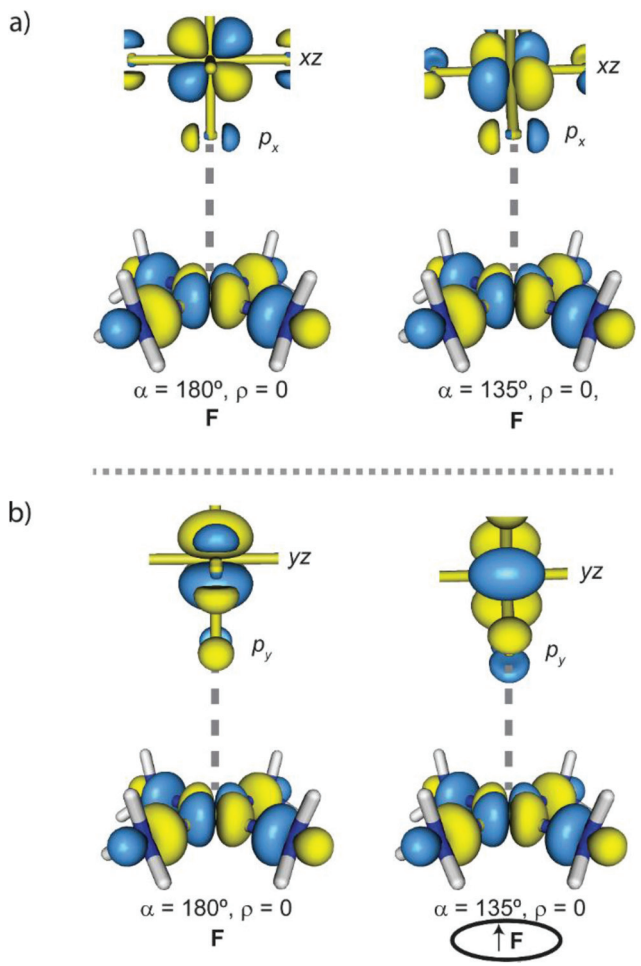

Fig. 8 The interaction between the d_{xz} (a) and d_{yz} (b) magnetic orbitals of the Re^{IV} ion with the $d_{x^2-y^2}$ orbital of the Cu^{II} ion. α is the Re–Cl–Cu angle and ρ the orbital overlap. The largest ferromagnetic exchange is found for α = 135°.

Table 3 Values of g_{Re}, D_{Re}, g_{Cu} and J parameters that provide the best-fit of the thermal dependence of $\chi_M T$ for **2–6**

Compound	g_{Re}	D_{Re}/cm^{-1}	g_{Cu}	J/cm^{-1}
2	1.804	−15.8	2.050	+0.11
3	1.778	−9.1	2.054	+1.59
4	1.807	−13.1	2.070	−0.12
5	1.764	−16.5	2.115	+2.16
6	1.814	−6.8	2.056	+0.33

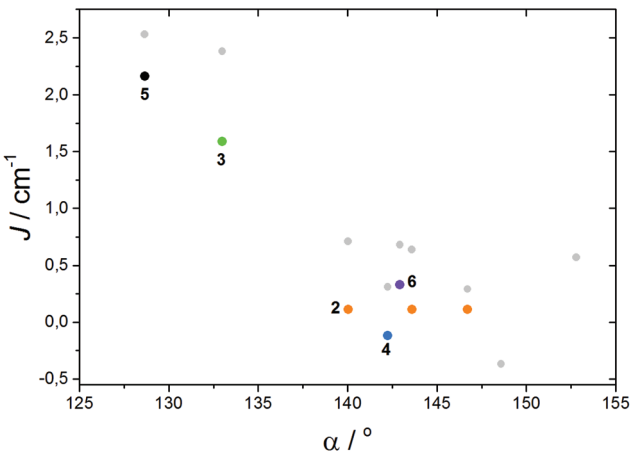

Fig. 9 The magnetic exchange parameters *versus* Re–Cl–Cu bridging angle. Points labelled in accordance with Table 3. Grey dots correlate to the values presented in Table 2.

Conclusions

A family of highly unusual one-dimensional chloro-bridged $Re^{IV}Cu^{II}$ chains has been built using the $[Re^{IV}Cl_6]^{2-}$ anion as a metalloligand. The complexes have been characterised structurally, magnetically and theoretically. Changing the nature (size/sterics) of the monodentate, terminally bonded ligand, L, on the Cu^{II} ions (L = imidazole (Imi, **1**), 1-methylimidazole (Meim, **2**), 1-vinylimidazole (Vim, **3**), 1-butylimidazole (Buim, **4**), 1-vinyl-1,2,4-triazole (Vtri, **5**) and *N*,*N*′-dimethylformamide (DMF, **6**)) and the subsequent changes to the packing of the chains in the crystal, results in the structures exhibiting significant intra-molecular differences in Cu–Cl bond lengths and Re–Cl–Cu bridging angles. This results in large differences in the nature and magnitude of magnetic exchange interactions between the Re^{IV} and Cu^{II} ions. Theoretical calculations show the coupling to be primarily ferromagnetic, with the developed magneto-structural correlation revealing that an increase in the magnitude of J occurs as the bridging angle becomes smaller and the bond lengths shorten.

Experimental

Materials and methods

All chemicals were used as received. Syntheses were carried out under aerobic conditions using CH_3CN dried over 3 Å molecular sieves. $(NBu_4)_2[ReCl_6]$ was prepared as described previously.[6,26] Crystals of the six compounds were collected and left open to air before use in further analysis. Elemental analyses (C, H, N) were performed by MEDAC Ltd. Direct current (dc) magnetic susceptibility measurements were collected on a Quantum Design MPMS-XL SQUID magnetometer equipped with a 7 T dc magnet in the temperature range 2.0–300 K. Diamagnetic corrections were applied using Pascal's constants.[27]

Crystallography

Data were measured on Rigaku Oxford Diffraction SuperNova (**1**, **2**, **5**, **6**) and Rigaku Oxford Diffraction XCalibur (**3**, **4**) X-ray diffractometers using Mo-K_α radiation. Structures were solved with olex2.solve (**1**, **2**, **6**)[28] or ShelXS (**3**, **4**, **5**)[29] and refined by full-matrix least-squares on *F*-squared using ShelXL, interfaced through Olex2.[30] In **1** C(18) is disordered over two positions with partial occupancies 0.74 and 0.26. In **3**, one vinyl-group is disorder over two positioned with partial occupancies 0.72 and 0.28. In **4**, the $-CH_2CH_3$ group of one ligand is disordered over two positions with partial occupancies 0.77 and 0.23. All non-hydrogen atoms were refined anisotropically. CCDC 1550271–1550276.†

Computational details

Calculations were performed with the Gaussian09 package using the CAM-B3LYP functional (a long range corrected version of B3LYP) and the quadratic convergence approach.[31–36] Double-ζ and Los Alamos effective core potentials, as proposed by Hay and Wadt, were used for the Re^{IV} and Cl^- ions.[37–39] Ahlrichs double-ζ basis set was used for the remaining atoms.[40] Two-electron integrals and their derivatives were computed from Douglas–Kroll–Hess (DKH) 2nd order scalar relativistic calculations.[41,42] An approach based on the use of broken-symmetry (BS) functions built from localised orbitals was employed to evaluate the energies of several spin states.[43] The BS functions were obtained from the guess functions generated with the fragment tool implemented in Gaussian09. Intermolecular magnetic couplings were calculated from the experimental structures. Intramolecular interactions were calculated on $Re^{IV}Cu^{II}$ models designed from experimental geometries. Parameters corresponding to the acetonitrile solvent were included to simulate the electronic effects of the surrounding molecules.[44] Calculations of the zero-field splitting, zfs, parameters were performed with version 3.0 of the ORCA program.[45] The TZVP basis set proposed by Ahlrichs, and tight SCF criteria were used in all cases.[40] Relativistic effects for the Re^{IV} ion were introduced from a zero-order regular approximation (ZORA).[46] For complete active space (CAS) calculations, this auxiliary basis set was replaced by TZV/C.[47,48] The zfs parameters were evaluated from N-Electron Valence State Perturbation Theory (NEVPT2) calculations and an approach based on an effective Hamiltonian for the spin–orbit coupling. This zfs calculation included contributions from ten quartet and twenty doublet states generated from electron promotion between d orbitals, which corresponds to the full active space modelled from only the five d orbitals of the Re^{IV} ion.[49–51]

Synthetic procedures

Synthesis of $\{[Cu(imidazole)_4][ReCl_6]\cdot 2^iPrOH\}_n$ (1). $(NBu_4)_2[ReCl_6]$ (0.05 mmol, 44.0 mg) and $Cu(NO_3)_2\cdot 3H_2O$ (0.05 mmol, 12.0 mg) were dissolved in 3 ml CH_3CN, to which imidazole (0.20 mmol, 13.6 mg) in 3 ml CH_3CN was added. Violet crystals suitable for single crystal X-ray diffraction were grown in 4 days from the solution by layering with isopropanol (53% yield). Elemental analysis (%) calculated (found) for $C_{12}H_{16}N_8Cl_6CuRe$: C, 19.6 (19.1); H, 2.2 (2.2); N, 15.3 (14.4).

Synthesis of $\{[Cu(1\text{-methylimidazole})_4][ReCl_6]\}_n$ (2). $(NBu_4)_2[ReCl_6]$ (0.05 mmol, 44.0 mg) and $Cu(NO_3)_2\cdot 3H_2O$ (0.05 mmol, 12.0 mg) were dissolved in 3 ml of acetonitrile at T = 4 °C to which 1-methylimidazole (0.20 mmol, 16.4 μl) in 3 ml of CH_3CN at T = 4 °C was added. Single crystals for X-ray diffraction were obtained from the solution after standing at T = 4 °C for 1 hour (85% yield). Elemental analysis (%) calculated (found) for $C_{16}H_{24}N_8Cl_6CuRe$: C, 24.3 (24.3); H, 3.1 (2.9); N, 14.2 (13.9).

Synthesis of $\{[Cu(1\text{-vinylimidazole})_4][ReCl_6]\}_n$ (3). $(NBu_4)_2[ReCl_6]$ (0.05 mmol, 44.0 mg) and $Cu(NO_3)_2\cdot 3H_2O$ (0.05 mmol, 12.0 mg) were dissolved in 5 ml of CH_3CN at T = 4 °C and subsequently 1-vinylimidazole (0.20 mmol, 19 μl) was added to the solution. Purple crystals suitable for single crystal X-ray diffraction were collected from the solution after standing at 4 °C for 1 hour (87% yield). Elemental analysis (%) cal-

culated (found) for $C_{20}H_{24}N_8Cl_6CuRe$: C, 28.6 (29.2); H, 2.9 (2.9); N, 13.4 (13.6).

Synthesis of {[Cu(1-butylimidazole)$_4$][ReCl$_6$]}$_n$ (4). $(NBu_4)_2[ReCl_6]$ (0.05 mmol, 44.0 mg) and $Cu(NO_3)_2{\cdot}3H_2O$ (0.05 mmol, 12.0 mg) were dissolved in 4 ml CH_3CN, then 1-butylimidazole (0.20 mmol, 26.2 μl) in 1 ml CH_3CN was added to the solution. Dark violet crystals suitable for diffraction were collected after exposing the solution to diethyl ether diffusion over a period of 2 weeks (56% yield). Elemental analysis (%) calculated (found) for $C_{28}H_{48}N_8Cl_6CuRe$: C, 35.1 (35.0); H, 5.0 (4.9); N, 11.7 (11.6).

Synthesis of {[Cu(1-vinyl-1,2,4-triazole)$_4$][ReCl$_6$]}$_n$ (5). $(NBu_4)_2[ReCl_6]$ (0.05 mmol, 44.0 mg) and $Cu(NO_3)_2{\cdot}3H_2O$ (0.05 mmol, 12.0 mg) were dissolved in 4 ml CH_3CN to which 1-vinyl-1,2,4-triazole (0.20 mmol, 19 μl) in 1 ml CH_3CN was added. Grey crystals suitable for X-ray diffraction were grown after 24 hours by layering with isopropanol (29% yield). Elemental analysis (%) calculated (found) for $C_{16}H_{20}N_{12}Cl_6CuRe$: C, 22.8 (23.0); H, 2.4 (2.4); N, 19.9 (19.4).

Synthesis of {[Cu(DMF)$_4$][ReCl$_6$]·CH$_3$CN}$_n$ (6). $(NBu_4)_2[ReCl_6]$ (0.05 mmol, 44.0 mg) and $Cu(NO_3)_2{\cdot}3H_2O$ (0.05 mmol, 12.0 mg) were dissolved in a mixture of 1 ml DMF and 1 ml CH_3CN. Green crystals suitable single crystal X-ray diffraction were grown after 24 hours by layering with isopropanol (74% yield). Elemental analysis (%) calculated (found) for $C_{12}H_{28}N_4O_4Cl_6CuRe$: C, 19.1 (19.0); H, 3.7 (3.5); N, 7.4 (7.3).

Acknowledgements

We thank the EPSRC (EKB), the Spanish Ministerio de Economía y Competitividad (MINECO) [projects CTQ2013-44844-P, CTQ2016-75068-P, CTQ2016-75671-P and MDM-2015-0538 (Excellence Unit "María de Maeztu")], and the Generalitat Valenciana (projects PROMETEO/2014/070 and ISIC/2012/002). JML thanks the Spanish MINECO for a "Ramon y Cajal" grant.

Notes and references

1 (*a*) K. S. Pedersen, A.-M. Ariciu, S. McAdams, H. Weihe, J. Bendix, F. Tuna and S. Piligkos, *J. Am. Chem. Soc.*, 2016, **138**, 5801; (*b*) M. A. Sørensen, H. Weihe, M. G. Vinum, J. S. Mortensen, L. H. Doerrer and J. Bendix, *Chem. Sci.*, 2017, **8**, 3566; (*c*) E. J. L. McInnes, G. A. Timco, G. F. S. Whitehead and R. E. P. Winpenny, *Angew. Chem., Int. Ed.*, 2015, **54**, 14244; (*d*) J. Ferrando-Soria, S. A. Magee, A. Chiesa, S. Carretta, P. Santini, I. J. Vitorica-Yrezabal, F. Tuna, G. F. S. Whitehead, S. Sproules, K. M. Lancaster, A.-L. Barra, G. A. Timco, E. J. L. McInnes and R. E. P. Winpenny, *Chemistry*, 2016, **1**, 727.

2 (*a*) M. D. Jenkins, D. Zueco, O. Roubeau, G. Aromí, J. Majer and F. Luis, *Dalton Trans.*, 2016, **45**, 16682; (*b*) M. Nakano and H. Oshio, *Chem. Soc. Rev.*, 2011, **40**, 3239; (*c*) K. L. Harriman and M. Murugesu, *Acc. Chem. Res.*, 2016, **49**, 1158; (*d*) A. J. Tasiopoulos and S. P. Perlepes, *Dalton Trans.*, 2008, 5537; (*e*) C. J. Milios and R. E. P. Winpenny, *Struct. Bonding*, 2015, **164**, 1.

3 J. Ferrando-Soria, J. Vallejo, M. Castellano, J. Martínez-Lillo, E. Pardo, J. Cano, I. Castro, F. Lloret, R. Ruiz-García and M. Julve, *Coord. Chem. Rev.*, 2017, **339**, 17.

4 X. Y. Wang, C. Avendano and K. R. Dunbar, *Chem. Soc. Rev.*, 2011, **40**, 3213.

5 (*a*) J. Martinez-Lillo, J. Faus, F. Lloret and M. Julve, *Coord. Chem. Rev.*, 2015, **289–290**, 215; (*b*) S. Kumar Singh and G. Rajaraman, *Nat. Commun.*, 2016, **7**, 10699.

6 R. Chiozzone, R. González, C. Kremer, G. De Munno, J. Cano, F. Lloret, M. Julve and J. Faus, *Inorg. Chem.*, 1999, **38**, 4745.

7 F. Pop, M. Allain, P. Auban-Senzier, J. Martinez-Lillo, F. Lloret, M. Julve, E. Canadell and N. Avarvari, *Eur. J. Inorg. Chem.*, 2014, 3855.

8 R. Gonzalez, F. Romero, D. Luneau, D. Armentano, G. De Munno, C. Kremer, F. Lloret, M. Julve and J. Faus, *Inorg. Chim. Acta*, 2005, **358**, 3995.

9 (*a*) T. D. Harris, M. V. Bennett, R. Clérac and J. R. Long, *J. Am. Chem. Soc.*, 2010, **132**, 3980; (*b*) S. Kumar Singh, K. R. Vignesh, V. Archana and G. Rajaraman, *Dalton Trans.*, 2016, **45**, 8201.

10 L. Arizaga, R. González, R. Chiozzone, C. Kremer, M. F. Cerdá, D. Armentano, G. D. Munno, F. Lloret and J. Faus, *Polyhedron*, 2008, **27**, 552.

11 A. Kochel, *Transition Met. Chem.*, 2010, **35**, 1.

12 J. Martinez-Lillo, D. Armentano, N. Marino, L. Arizaga, R. Chiozzone, R. Gonzalez, C. Kremer, J. Cano and J. Faus, *Dalton Trans.*, 2008, 4585.

13 M. V. Bennett and J. R. Long, *J. Am. Chem. Soc.*, 2003, **125**, 2394.

14 D. E. Freedman, D. M. Jenkins, A. T. Iavarone and J. R. Long, *J. Am. Chem. Soc.*, 2008, **130**, 2884.

15 J. M. Zadrozny, D. E. Freedman, D. M. Jenkins, T. D. Harris, A. T. Iavarone, C. Mathonière, R. Clérac and J. R. Long, *Inorg. Chem.*, 2010, **49**, 8886.

16 J. Martínez-Lillo, D. Armentano, G. De Munno, W. Wernsdorfer, M. Julve, F. Lloret and J. Faus, *J. Am. Chem. Soc.*, 2006, **128**, 14218.

17 L. Arizaga, R. González, D. Armentano, G. De Munno, M. A. Novak, F. Lloret, M. Julve, C. Kremer and R. Chiozzone, *Eur. J. Inorg. Chem.*, 2016, 1835.

18 J. Martinez-Lillo, D. Armentano, G. De Munno, N. Marino, F. Lloret, M. Julve and J. Faus, *CrystEngComm*, 2008, **10**, 1284.

19 D. Armentano and J. Martinez-Lillo, *Inorg. Chim. Acta*, 2012, **380**, 118.

20 K. S. Pedersen, M. Sigrist, M. A. Sørensen, A.-L. Barra, T. Weyhermüller, S. Piligkos, C. A. Thuesen, M. G. Vinum, H. Mutka, H. Weihe, R. Clérac and J. Bendix, *Angew. Chem., Int. Ed.*, 2014, **53**, 1351.

21 J. Martinez-Lillo, D. Armentano, G. De Munno, F. Lloret, M. Julve and J. Faus, *Dalton Trans.*, 2008, 40.

22 J. Martinez-Lillo, J. Kong, W. P. Barros, J. Faus, M. Julve and E. K. Brechin, *Chem. Commun.*, 2014, **50**, 5840.

23 N. Marino, D. Armentano, G. De Munno, F. Lloret, J. Cano and M. Julve, *Dalton Trans.*, 2015, **44**, 11040.
24 P. J. Hay, J. C. Thibeault and R. Hoffmann, *J. Am. Chem. Soc.*, 1975, **97**, 4884.
25 O. Kahn, *Molecular Magnetism*, VCH Publisher, Inc., 1993.
26 J. Kleinberg, *Inorg. Synth*, McGraw-Hill, 1963.
27 G. A. Bain and J. F. Berry, *J. Chem. Educ.*, 2008, **85**, 532.
28 L. J. Bourhis, O. V. Dolomanov, R. J. Gildea, J. A. K. Howard and H. Puschmann, *Acta Crystallogr., Sect. A: Fundam. Crystallogr.*, 2015, **71**, 59.
29 G. Sheldrick, *Acta Crystallogr., Sect. A: Fundam. Crystallogr.*, 2008, **64**, 112.
30 O. V. Dolomanov, L. J. Bourhis, R. J. Gildea, J. A. K. Howard and H. Puschmann, *J. Appl. Crystallogr.*, 2009, **42**, 339.
31 M. J. Frisch, *et al.*, Gaussian, Inc., Wallingford CT, 2009.
32 A. D. Becke, *Phys. Rev. A*, 1988, **38**, 3098.
33 A. D. Becke, *J. Chem. Phys.*, 1993, **98**, 5648.
34 C. Lee, W. Yang and R. G. Parr, *Phys. Rev. B: Condens. Matter*, 1988, **37**, 785.
35 T. Yanai, D. P. Tew and N. C. Handy, *Chem. Phys. Lett.*, 2004, **393**, 51.
36 A. Schäfer, H. Horn and R. Ahlrichs, *J. Chem. Phys.*, 1992, **97**, 2571.
37 P. J. Hay and W. R. Wadt, *J. Chem. Phys.*, 1985, **82**, 270.
38 W. R. Wadt and P. J. Hay, *J. Chem. Phys.*, 1985, **82**, 284.
39 P. J. Hay and W. R. Wadt, *J. Chem. Phys.*, 1985, **82**, 299.
40 A. Schäfer, C. Huber and R. Ahlrichs, *J. Chem. Phys.*, 1994, **100**, 5829.
41 M. Douglas and N. M. Kroll, *Ann. Phys.*, 1974, **82**, 89.
42 B. A. Hess, *Phys. Rev. A*, 1985, **32**, 756.
43 E. Ruiz, J. Cano, S. Alvarez and P. Alemany, *J. Comput. Chem.*, 1999, **20**, 1391.
44 J. Tomasi, B. Mennucci and E. Cancès, *J. Mol. Struct. (THEOCHEM)*, 1999, **464**, 211.
45 F. Neese, *Wiley Interdiscip. Rev.: Comput. Mol. Sci.*, 2012, **2**, 73.
46 C. Ch, M. Pelissier and D. Ph, *Phys. Scr.*, 1986, **34**, 394.
47 K. Eichkorn, O. Treutler, H. Öhm, M. Häser and R. Ahlrichs, *Chem. Phys. Lett.*, 1995, **242**, 652.
48 K. Eichkorn, F. Weigend, O. Treutler and R. Ahlrichs, *Theor. Chem. Acc.*, 1997, **97**, 119.
49 C. Angeli, R. Cimiraglia, S. Evangelisti, T. Leininger and J.-P. Malrieu, *J. Chem. Phys.*, 2001, **114**, 10252.
50 C. Angeli, R. Cimiraglia and J.-P. Malrieu, *Chem. Phys. Lett.*, 2001, **350**, 297.
51 C. Angeli, R. Cimiraglia and J.-P. Malrieu, *J. Chem. Phys.*, 2002, **117**, 9138.